Environmental Research 228 (2023) 115930

Contents lists available at ScienceDirect

Environmental Research

journal homepage: www.elsevier.com/locate/envres

Combination of adsorption/desorption and photocatalytic reduction processes for PFOA removal from water by using an aminated biosorbent and a UV/sulfite system

Zhongfei Ren [a,*], Ulrich Bergmann [b], Jean Noel Uwayezu [c], Ivan Carabante [c], Jurate Kumpiene [c], Tore Lejon [c,d], Tiina Leiviskä [a]

[a] Chemical Process Engineering, University of Oulu, P.O. Box 4300, FIN-90014, Oulu, Finland
[b] Department of Biochemistry and Biocenter, University of Oulu, Oulu, FIN-99020, Finland
[c] Waste Science and Technology, Luleå University of Technology, Luleå, Sweden
[d] Department of Chemistry, UiT-The Arctic University of Norway, Norway

ARTICLE INFO

Handling Editor: Aijie Wang

Keywords:
Perfluorooctanoic acid
Advanced reduction process
Adsorption/ desorption
Biomass sorbent
UV/Sulfite system

ABSTRACT

Per- and polyfluoroalkyl substances (PFAS) are stable organic chemicals, which have been used globally since the 1940s and have caused PFAS contamination around the world. This study explores perfluorooctanoic acid (PFOA) enrichment and destruction by a combined method of sorption/desorption and photocatalytic reduction. A novel biosorbent (PG-PB) was developed from raw pine bark by grafting amine groups and quaternary ammonium groups onto the surface of bark particles. The results of PFOA adsorption at low concentration suggest that PG-PB has excellent removal efficiency (94.8%–99.1%, PG-PB dosage: 0.4 g/L) to PFOA in the concentration range of 10 μg/L to 2 mg/L. The PG-PB exhibited high adsorption efficiency regarding PFOA, being 456.0 mg/g at pH 3.3 and 258.0 mg/g at pH 7 with an initial concentration of 200 mg/L. The groundwater treatment reduced the total concentration of 28 PFAS from 18 000 ng/L to 9900 ng/L with 0.8 g/L of PG-PB. Desorption experiments examined 18 types of desorption solutions, and the results showed that 0.05% NaOH and a mixture of 0.05% NaOH + 20% methanol were efficient for PFOA desorption from the spent PG-PB. More than 70% (>70 mg/L in 50 mL) and 85% (>85 mg/L in 50 mL) of PFOA were recovered from the first and second desorption processes, respectively. Since high pH promotes PFOA degradation, the desorption eluents with NaOH were directly treated with a UV/sulfite system without further adjustment. The final PFOA degradation and defluorination efficiency in the desorption eluents with 0.05% NaOH + 20% methanol reached 100% and 83.1% after 24 h reaction. This study proved that the combination of adsorption/desorption and a UV/sulfite system for PFAS removal is a feasible solution for environmental remediation.

1. Introduction

Per- and poly-fluoroalkyl substances (PFAS) have been widely used globally, leading to extensive contamination around the world (Li et al., 2020; Xu et al., 2021). Due to the high stability of the C–F bond, PFAS are extremely resistant to oxidation and are recognized as persistent pollutants. Besides, PFAS have been proven to have significant bio-accumulation effects and toxicity to the environment (Ghisi et al., 2019; Helmer et al., 2022). It has been reported that the serum perfluorooctanesulfonate (PFOS) concentration (889 ± 56 ng/mL) of turtles exposed to PFAS-contaminated water was 235 times higher than that in the contaminated site (ΣPFAS 32.0 μg/L) (Beale et al., 2022). In addition, PFAS have also been detected in human urine, blood, nails, hair and breast milk (Jian et al., 2018; Macheka-Tendenguwo et al., 2018). Human exposure to PFAS has been proven to be associated with many diseases, such as kidney cancer, testicular cancer and thyroid disease (Jian et al., 2018; Sunderland et al., 2019). Perfluorooctanoic acid (PFOA) and PFOS are two representative PFAS listed as persistent organic pollutants (POPs) in the Stockholm Convention to limit their production and application (Stockholm Convention, 2019). In June 2022, the US Environmental Protection Agency (USEPA) issued an interim updated health advisory for PFOA and PFOS in drinking water,

* Corresponding author.
E-mail address: zhongfei.ren@oulu.fi (Z. Ren).

https://doi.org/10.1016/j.envres.2023.115930
Received 19 January 2023; Received in revised form 4 April 2023; Accepted 15 April 2023
Available online 17 April 2023

which recommends a level of 0.004 parts per trillion (ppt) for PFOA and 0.02 ppt for PFOS (US EPA, 2022). Thus, it is critical to develop effective techniques for purification water contaminated with PFAS.

In recent decades, various destructive technologies, such as advanced oxidation processes (AOPs), advanced reduction processes (ARPs), electrocatalysis and photodecomposition, have been investigated for the elimination of PFAS (cleavage of the C–F bond) from water (Lu et al., 2020; Uwayezu et al., 2021). Among these techniques, AOPs have shown good degradation performance for PFAS. However, AOPs typically do not completely degrade long-chain PFAS, leading to the formation of more stable short-chain PFAS and resulting in low defluorination efficiency. (Chen and Zhang, 2006; Qian et al., 2016). In contrast, ARPs have exhibited much higher defluorination (up to 99%) and decomposition efficiency (up to 100%) by cleaving C–F bonds with highly reactive radicals and hydrated electrons (e^-_{aq}, $E = -2.9$ V) (Bentel et al., 2019; Ren et al., 2021). Hydrated electrons can be generated from water or from certain source chemicals such as iodide, sulfite or indole under UV radiation. (Guo et al., 2019). Among these, sulfite has been recognized as a good reductant for PFAS degradation by ARPs due its high efficiency and robustness. For example, in the study by Song et al. (2013), PFOA was totally degraded by the UV/sulfite system in 1 h and the defluorination ratio reached 88.5% after 24 h (Song et al., 2013). Our recent study has shown that the UV/sulfite system works efficiently even with high concentrations of coexisting compounds (1.709 M of chloride, 5 mM of carbonate, 5 mM of phosphate and 10 mg/L of humic acid) (Ren et al., 2021). However, the concentration of PFAS reported in contaminated waters is usually too low (ng to μg/L level) to be directly treated by ARPs (Li et al., 2020; Rahman et al., 2014). Therefore, pretreatment methods are required to concentrate PFAS before applying ARPs.

The common separation technologies applied for PFAS removal include surface-active foam fractionation (SAFF) (Burns et al., 2021), membrane treatment (Lee et al., 2022) and sorption (Boyer et al., 2021a). Of the various separation methods, sorption is a well-studied approach for removing PFAS due to its relatively low cost and ease of operation. The most investigated sorbents include activated carbon (AC), commercial resins and biosorbents. AC is one of the most versatile and cost-effective adsorbents applied for PFAS treatment (Yuan et al., 2022). However, despite the high adsorption capacity in relation to PFAS, the regeneration of spent ACs by conventional desorption eluents is challenging (Du et al., 2014). One possible method for the regeneration of ACs is to use high temperature to decompose the adsorbed PFAS, although this consumes more energy. For example, DiStefano et al. reported the reactivation of PFAS laden granular activated carbon (GAC) by thermal treatment at 1650–2000 °F (899–1093 °C), which achieved >99.99% of PFAS destruction (DiStefano et al., 2022). An alternative choice to ACs is anion exchange resins (AER), which was reported to remove both long- and short-chain PFAS efficiently in various concentrations (Boyer et al., 2021a). Moreover, the regeneration of PFAS laden resins by various salt solutions (e.g. NaCl, NaOH, NH_4Cl, methanol and ethanol) has been proved to be efficient. In Dixit et al.'s study, 10% NaCl solution (W/V) was used for PFAS desorption from Purolite® A860, which resulted in 94% and 90% recovery of PFOA and PFOS, respectively (Dixit et al., 2020). Aminated biosorbents are environmentally sustainable and cost-effective alternatives to AER, as the raw materials are renewable and abundantly available (Vu and Wu, 2020). In the study by Deng et al. aminated rice husk was prepared and used for the removal of PFOA, perfluorobutanoic acid (PFBA) and PFOS from water, with a sorption capacity of 2.49, 1.70 and 2.65 mmol/g, respectively (Deng et al., 2013). Although aminated biosorbents have been widely investigated for anion removal, studies related to PFAS sorption/desorption by aminated biosorbents remain limited. Therefore, the development of efficient biosorbent and desorption methods is essential to achieve sustainable workflows for PFAS removal by a combined method of sorption/desorption and ARPs.

In this study, a combination of sorption/desorption and a photocatalytic reduction system was successfully applied for PFOA removal. A novel biosorbent (PG-PB) was synthesized from pine bark with surface modification using polyethylenimine (PEI) and glycidyltrimethylammonium chloride (GTMAC). The properties of PG-PB were analysed, and its adsorption kinetics, isotherms, and the effects of pH on PFOA removal were investigated. Then this study focused on testing various desorption solutions for PG-PB regeneration, which would allow the reuse of the adsorbent and reduce disposal problems. The resulting PFOA-rich effluent was directly treated with the UV/sulfite system in order to permanently destroy the PFOA.

2. Materials and methods

2.1. Chemicals and reagents

Sodium chloride, sulfuric acid, sodium hydroxide, hydrochloric acid, absolute ethanol and methanol were purchased from VWR. Sodium sulfite, polyethylenimine (PEI, ≥99%, Mw 25 000 by LS, branched) and glycidyltrimethylammonium chloride (GTMAC, ≥90%), trifluoroacetic acid (TFA, >99.0%), pentafluoropropionic acid (PFPrA, >98%), heptafluorobutyric acid (PFBA, >99%), nonafluoropentanoic acid (PFPeA, >98%), undecafluorohexanoic acid (PFHxA, >98%), tridecafluoroheptanoic acid (PFHpA, >96%) and PFOA (>95%) were all purchased from Sigma-Aldrich. The fluoride ionic strength adjustment (ISA) powder pillows and fluoride standard solutions (0.5, 1 and 2 mg/L) from Hach were used for fluoride analysis. A stock solution of PFOA (2 g/L) was prepared by dissolving PFOA in Milli-Q water (Merck Millipore). HCl, NaOH and H_2SO_4 solutions were used for pH adjustment. Unless otherwise specified, all chemicals used were of analytical grade.

The raw material, pine bark (PB), was collected from the RoihuPuu Company (Oulu, Finland). After drying at 80 °C for 24 h, the dried PB was then ground and sieved to obtain a 90–250 μm fraction for further modification. The groundwater sample was collected close to a hot spot where PFAS that contained aqueous film forming foams (FFF) had been applied in firefighting training activities.

2.2. Preparation of PEI-GTMAC modified pine bark (PG-PB)

The modification of pine bark was done in two steps by using a method previously developed for peat biomass (Gogoi et al., 2019): 1) Firstly, 4 g of pine bark particles were soaked in 40 mL water with continuous stirring. The mixture was then heated to 60 °C, followed by the addition of 10 g of PEI; stirring was continued for 6 h. After that, the intermediate product (PEI-PB) was cooled down to room temperature and washed with Milli-Q water several times to remove the extra PEI. 2) Next, the wet PEI-PB was soaked in 40 mL 2 g/L NaOH solution and heated to 60 °C with stirring. Then, 5 mL of GTMAC was added into the mixture and stirring was continued for 6 h. The product (PG-PB) was filtered and washed with Milli-Q water several times to remove extra chemicals. Finally, the wet PG-PB was dried at 80 °C for 24 h and stored for further use.

2.3. Characterization of PG-PB

To understand the physical and chemical properties of the biosorbent, the raw pine bark (PB), PEI-modified pine bark (PEI-PB) and PEI-GTMAC-modified pine bark (PG-PB) were characterized by Brunauer-Emmett-Teller (BET) surface area analysis, Barrett-Joyner-Halenda (BJH) pore size and volume analysis, SEM, FTIR and XPS. The surface compositions and chemical bonding of PB, PEI-PB, PG-PB and spent PG-PB were analysed by XPS (Thermo Fisher Scientific ESCALAB 250Xi). The specific surface areas and pore size distributions of PB, PEI-PB and PG-PB were obtained by N_2 adsorption using the ASAP^{TM} 2020 Accelerated Surface Area and Porosimetry system (Micromeritics) with the Brunauer-Emmett-Teller (BET) and Barrett-Joyner-Halenda (BJH) methods. The morphology, particle size and

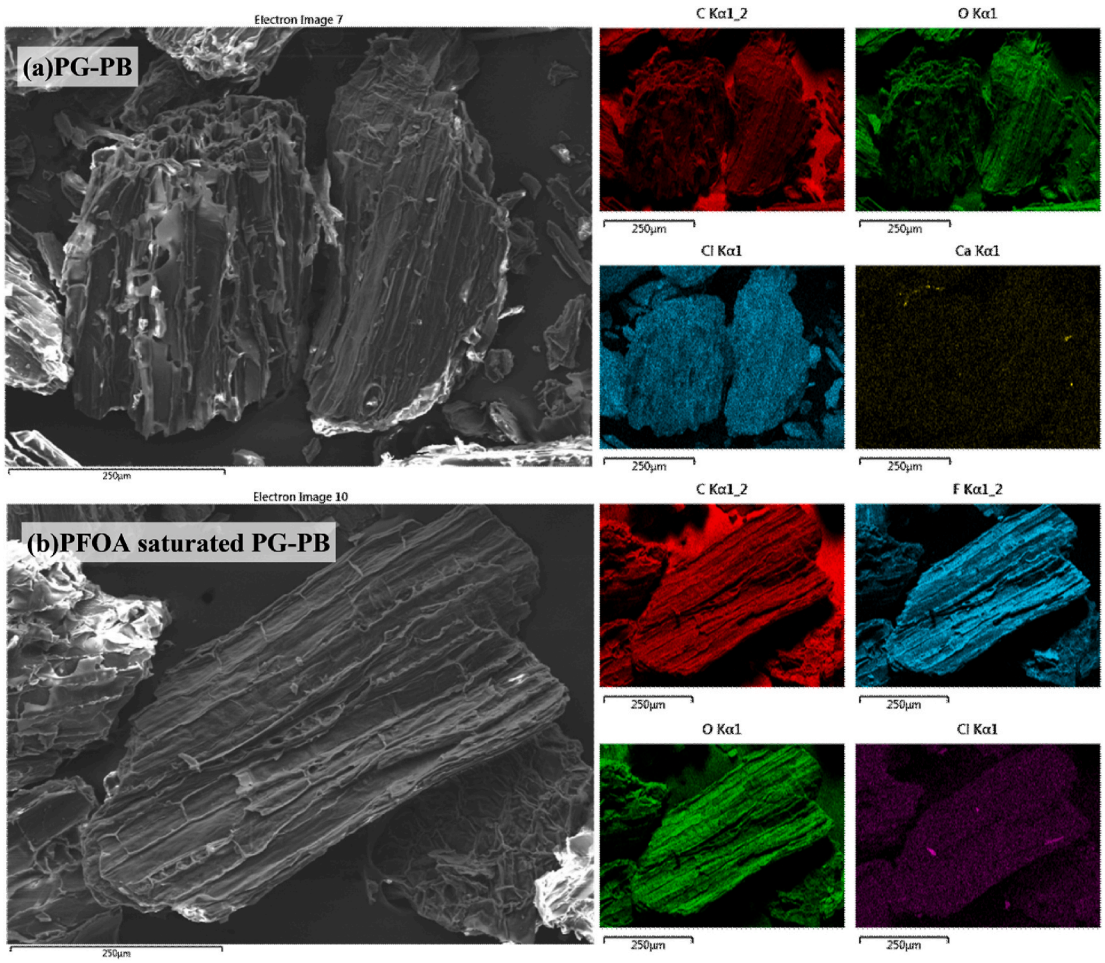

Fig. 1. EDS mapping of a) PG-PB and b) PFOA-saturated PG-PB.

elemental distribution of PB and PG-PB were analysed with a field emission scanning electron microscope (FESEM, Zeiss Ultra Plus), equipped with an energy-dispersive X-ray spectroscopy (EDS) detector. Functional groups on PB, PEI-PB, PG-PB and PFOA-saturated PG-PB were analysed with a Fourier-transform infrared (FTIR) spectrometer (Bruker, Vertex V80/DRIFT).

2.4. Adsorption and desorption of PFOA

The adsorption and desorption tests were carried out in 50 mL centrifuge tubes. In a typical adsorption or desorption test, 0.02 g of PG-PB was introduced into a 50 mL solution (dosage: 0.4 g/L) in a centrifuge tube and mixed using tube rotators (Fisherbrand™ Multi-Purpose Tube Rotators) at 25 rpm. The adsorption of PFOA at low concentration was performed without pH adjustment at initial PFOA concentrations of 0.01, 0.05, 0.1, 0.15, 0.2, 0.5, 1, 1.5 and 2 mg/L. The effect of pH on PFOA adsorption (200 mg/L) was studied at 10 different pH values (2, 3, 4, 5, 6, 7, 8, 9, 10 and 11) to determine the optimal pH conditions for PG-PB. The adsorption kinetic experiments were conducted in 200 mg/L PFOA solution at pH 3.3 with different time intervals (5, 10, 20, 30, 45, 60, 120, 180, 240, 300, 360 and 540 min). The adsorption isotherm experiments were carried out with PFOA concentrations of 10, 20, 60, 100, 200, 400, 600 and 1000 mg/L for 24 h, at pH 3.3. The analytical methods for PFOA are given in the supporting information. For the desorption experiments, NaOH, NaCl, methanol and mixtures of them (mixture details are provided in Section 3.6) were used as the regeneration solution and the desorption efficiencies of PFOA were measured. The best performing regeneration solution was selected and used for further experiments. All samples were filtered through a 0.45 μm membrane (VWR, polyethersulfone) to remove small particles of PG-PB before the PFOA analysis.

The pseudo first order (Lagergren, 1898), pseudo second order (Blanchard et al., 1984), intra-particle diffusion (Weber and Morris, 1963), Boyd (Boyd et al., 1947) and Elovich (McLintock, 1967) equations were employed to fit the experimental data of the PFOA adsorption kinetics. The non-linear Langmuir (1918), Freundlich (1907), Redlich-Peterson (Redlich and Peterson, 1959) and Dubinin-Radushkevich (Dubinin, 1947) equations were applied to fit the experimental data of the PFOA adsorption isotherm. The expressions of the equations are listed in the supporting information in Section S1.

The column study was done in transparent polymethyl methacrylate (PMMA) columns connected to a peristaltic pump. The inner diameter of the columns was 10 mm, and the height was 150 mm. The weight of the filled PG-PB was 0.4 g and the height was around 40 mm. The columns were filled with quartz sand before and after filling the sorbent to maintain a good hydraulic property. Two PFOA solutions with different concentrations, 40 mg/L and 80 mg/L (without pH adjustment), were selected as the feed solution. The flow rate was 0.2 mL/min and the temperature was 21 °C. Due to the high adsorption capacity of PG-PB, the sampling interval was set to 3 h during the day, and 6 h during the night. The Thomas model (Chu, 2010) was used to fit the column adsorption data.

The PFAS-contaminated groundwater was used for the batch adsorption tests to evaluate the PFAS removal efficiency by the PG-PB. All the adsorption experiments were done in 250 mL centrifuge bottles in a rotary mixer for 24 h at room temperature (21 °C). The PG-PB

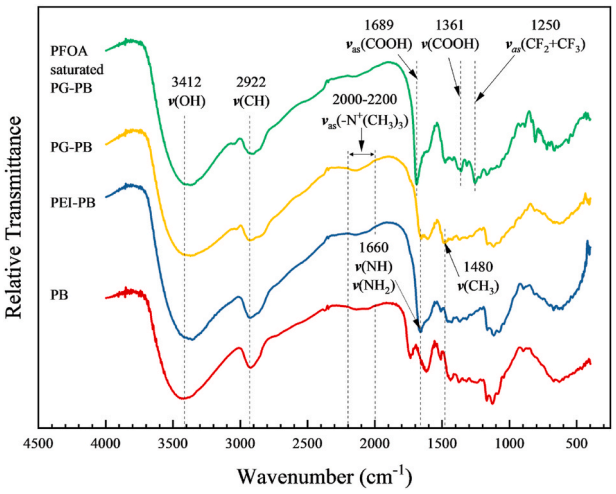

Fig. 2. FTIR spectra of PB, PEI-PB, PG-PB and PFOA-saturated PG-PB.

dosages were 0.4 g/L and 0.8 g/L. Before sampling, all treated samples were filtered with a filter paper to remove particles. The groundwater samples were analysed by Eurofins Food & Feed Testing Sweden AB.

2.5. UV/sulfite treatment for desorption effluent

A cylindrical glass container (78 mm in diameter and 270 mm in height) was used as the UV degradation reactor. A UV lamp (TUV PL-S 11 W, 254 nm, Philips) was packed in a quartz tube and placed in the centre of the reactor. Experiments were conducted at room temperature (21 °C). To obtain the desorption effluent, the adsorption experiments were firstly conducted in 100 mg/L PFOA solution with 0.4 g/L PG-PB for 24 h, then the spent PG-PB was regenerated with 500 mL of 0.05% NaOH solution and a mixture of 0.05% NaOH +20% MeOH for 4 h (solid: liquid = 1 : 2500). Finally, the desorption effluent was collected and subjected to photocatalytic degradation. To investigate the effect of the concentration on degradation performance, two desorption effluents were diluted 10 times before UV/sulfite degradation, whereas the UV/sulfite system was applied directly to two desorption effluents. The dosage of sulfite was 10 mM and pH was measured by a pH meter (inoLab® pH 7110).

3. Results and discussion

3.1. SEM, BET-BJH and EDS analysis

SEM analysis was performed to investigate the morphology of the biosorbent. The FESEM images of PB, PEI-PB, PG-PB and PFOA-saturated PG-PB showed that the surface modification and introduction of PFOA did not cause any visible changes to the surface of the pine bark particles (Fig. S1). However, the BET-BJH analysis showed that the SSA and total pore volume were reduced after surface modification (Table S1). This could be attributed to the reaction between PEI, GTMAC and the PB surface that blocked the microporous structure, as the average pore diameter increased from 17.69 nm to 72.36 nm after GTMAC modification. The low SSA of PG-PB (0.2387 m^2/g) also indicated that the SSA is not the key factor governing the PFOA adsorption. The EDS and EDS mapping results are given in Fig.S2 and Fig. 1. The EDS results for PG-PB show that the Cl content increased to 9.85%, which was in agreement with the XPS results (Section 3.3, Fig. S5). Besides, the

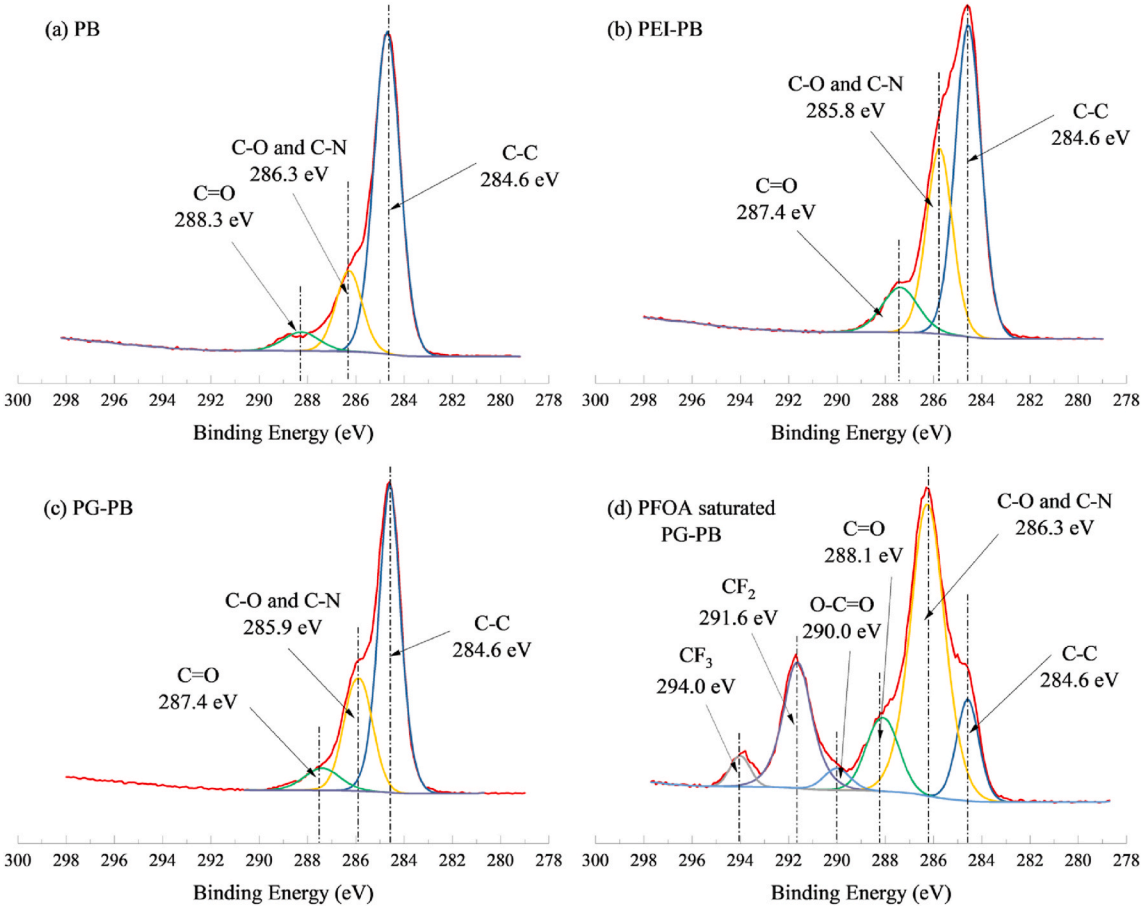

Fig. 3. C 1s XPS spectra of a) PB, b) PEI-PB, c) PG-PB and d) PFOA-saturated PG-PB.

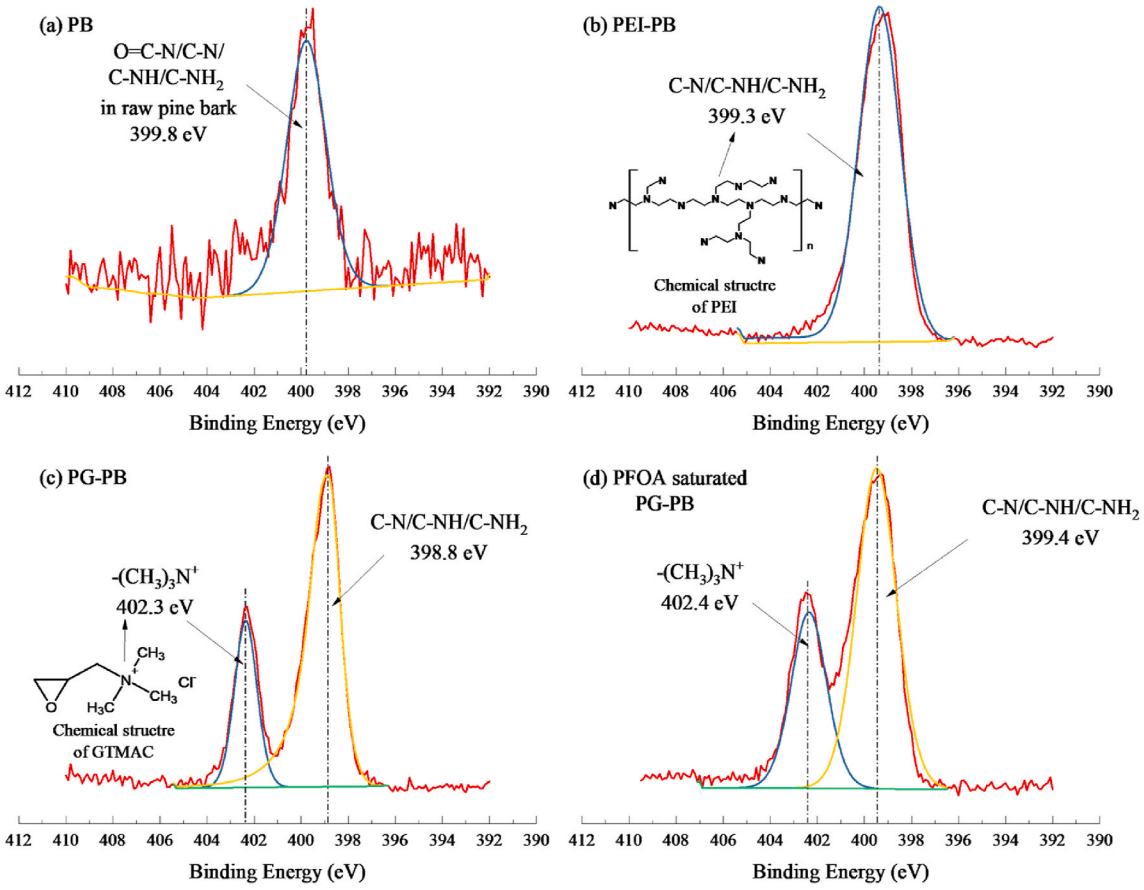

Fig. 4. N 1s XPS spectra of a) PB, b) PEI-PB, c) PG-PB and (d) PFOA-saturated PG-PB.

EDS mapping (Fig. 1a) shows that Cl was distributed homogeneously on the PG-PB surface. This result indicates that the quaternary ammonium groups were successfully grafted onto the surface of the biosorbent after GTMAC modification. After the adsorption of PFOA, dense EDS signals of F were observed on the surface of the PFOA-saturated PG-PB (Fig. 1b), and the F content increased to 37.4% while the Cl content dropped to 0.76% (Fig. S2). It can be deduced from the above results that the ion exchange between Cl^- and PFOA anions is one of the predominant adsorption mechanisms.

3.2. FTIR analysis

The FTIR spectra of PB, PEI-PB, PG-PB and PFOA-saturated PG-PB are shown in Fig. 2. The broad band at 3412 cm^{-1} is associated with the hydroxyl group and hydrogen bonds (Fleming et al., 2019). The stretching vibration of C–H presents a strong peak at 2922 cm^{-1}, which derives from the natural lignin-containing materials (Herbert, 1960). After PEI modification, a band appeared at 1660 cm^{-1}, which was attributed to the N–H bending vibration from the large amount of amine groups derived from PEI (Sowmya and Meenakshi, 2014). However, in PG-PB, the peak at 1660 cm^{-1} had shrunk significantly due to the reaction of amine groups and GTMAC, which linked the quaternary ammonium groups onto the biosorbent (Gogoi et al., 2019). The band observed in the PG-PB spectrum at 1480 cm^{-1} was assigned to the symmetric stretching vibration of $–CH_3$ group from quaternary ammonium (Ren et al., 2017). In addition, the broad band located at 2000-2200 cm^{-1} was assigned to the asymmetrical bending vibration of the quaternary ammonium group ($–N^+(CH_3)_3$) and the torsional oscillation of the trimethylammonium group (Zou et al., 2015). This corresponded well to the XPS results (Fig. 4c) as quaternary ammonium groups were detected in the N 1s spectrum. The band at 1361 cm^{-1} is in accordance with the single bond –OH bending vibration (Li et al., 2015), which is derived from the –COOH group of PFOA. In addition, the strong peak at 1689 cm^{-1} is ascribed to the stretching vibration of –C═O and –COOH in the carbonyl groups (Lin et al., 2015; Xu et al., 2015), which is in line with the XPS results and the high amount of PFOA. The sharp band at 1250 cm^{-1} was assumed to correspond to the C–F vibration of PFOA (Lin et al., 2015; Xu et al., 2015). To summarize, FTIR analysis confirmed the successful surface modification of PG-PB by PEI and GTMAC, and high PFOA adsorption on the surface.

Table 1
Peak table of PB, PEI-PB, PG-PB and PFOA-saturated PG-PB from XPS survey.

Sample	Name	peak BE (eV)	Atomic %
PB	C 1s	284.9	83.3
	O 1s	532.6	16.2
	N 1s	401.7	0.5
PEI-PB	C 1s	285.2	75.1
	O 1s	532.2	15.6
	N 1s	399.6	9.8
PG-PB	C 1s	285.2	80.4
	O 1s	532.3	12.6
	N 1s	399.9	6.1
	Cl 2p	197.8	1.0
PFOA-saturated PG-PB	C 1s	286.8	41.3
	O 1s	532.8	11.0
	N 1s	401.4	5.2
	F 1s	689.8	42.3
	Cl 2p	199.0	0.2

3.3. XPS analysis

The XPS survey spectra are shown in Fig. S4. The C 1s, N 1s, Cl 2p and

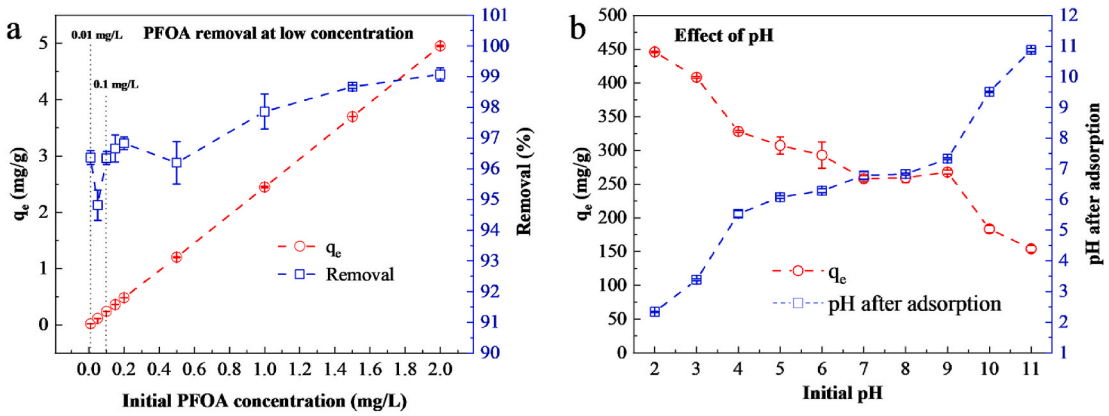

Fig. 5. a) PFOA removal at low concentration (pH = 5.2); b) Effect of pH on PFOA adsorption (Initial PFOA concentration = 200 mg/L); (PG-PB dosage: 0.4 g/L, contact time = 24 h, T = 21 °C).

F 1s high-resolution spectra of PB, PEI-PB, PG-PB and PFOA-saturated PG-PB, are given in Figs. 3–4 and Fig. S5-S6. The main elements observed on the PB surface (Table 1) were carbon (83.3%), oxygen (16.2%) and nitrogen (0.46%). After PEI modification and GTMAC modification, the atomic percentages of N in PEI-PB and PG-PB had greatly increased, to 9.8% and 6.1%, respectively. Besides, a Cl 2p peak was also detected for the PG-PB sample. These results indicate that the amine group and quaternary ammonium had been successfully grafted onto the biomass surface. The strong F 1s peak observed in the XPS survey of PFOA-saturated PG-PB (42.3%, Table 1) suggests that PG-PB has a high adsorption capacity for PFOA.

The C 1s spectra of the four samples are shown in Fig. 3. The C 1s spectrum of PB showed three peaks (Fig. 3a) at 284.6 eV, 286.3 eV and 288.3 eV, which could be assigned to the C–C, C–O/C–N and C═O bonds in the PB (Su et al., 2022). After PEI modification, the peaks at 285.8 eV and 287.4 eV (Fig. 3b) were attributed to the C–N/C–O and C═O groups. The same peaks were also observed in the PG-PB sample (Fig. 3c), which suggests that the grafting of amine and quaternary ammonium groups had been achieved. Two intensive peaks were observed at 294.0 eV and 291.6 eV in the PFOA-saturated PG-PG sample (Fig. 3d), which could be attributed to the CF_3 and CF_2 components of PFOA (Liu et al., 2018). In addition, the peak at 290.0 eV probably originated from the O–C═O group of PFOA. The above results indicate the successful adsorption of PFOA on the PG-PB surface, which is also consistent with the FTIR results.

The peak at 399.8 eV in the N 1s spectrum originated from the organic nitrogen in the raw pine bark (Fig. 4a). After PEI modification, the C–N peak shifted to 399.3 eV (Fig. 4b), and the proportion of nitrogen increased dramatically (Table 1). This could be attributed to the large amounts of primary amine (-NH_2 group), secondary amine (-$(CH_x)_2NH$ group) and tertiary amine groups (-$(CH_x)_3N$ group) from the PEI (Fig. S3a) modification (Gogoi et al., 2019). The new peak at 402.3 eV in the N 1s spectrum (Fig. 4c) of PG-PB can be ascribed to the quaternary ammonium groups (-$(CH_3)_3N^+Cl^-$) after GTMAC modification (Gogoi et al., 2019; Cao et al., 2016). For PFOA-saturated PG-PB, the C–N peak shifted from 398.8 eV to 399.4 eV. This is probably due to the adsorption of PFOA by amine groups that changed the properties of the C–N bond.

The Cl 2p XPS spectra are shown in Fig. S5. In the PB and PEI-PB samples, no Cl 2p peak was detected (Fig. S5a, b). After GTMAC modification, the Cl $2p_{1/2}$ and Cl $2p_{3/2}$ peaks were observed at 198.7 and 197.0 eV in the PG-PB (Fig. S5c) and the binding energy separation between Cl $2p_{1/2}$ and Cl $2p_{3/2}$ peaks was 1.7 eV, which can be related to the chloride on the quaternary ammonium groups (-$(CH_3)_3N^+Cl^-$) (Ren et al., 2015). After PFOA adsorption, the atomic percentage of Cl dropped from 0.97% to 0.24%. In addition, a strong peak at 688.9 eV was observed in the F 1s spectrum (Fig. S6d), which implies that ion exchange was partly responsible for PFOA adsorption. However, as the NaCl solution was not effective for PFOA desorption (Section 3.6), and the PG-PB achieved an extremely high adsorption capacity for PFOA (Section 3.4), this implies that other adsorption mechanisms such as hydrophobic, electrostatic attraction and PFOA self-aggregation contribute to the adsorption. A detailed discussion is given in Sections 3.4 and 3.6.

3.4. Adsorption of PFOA

3.4.1. PFOA removal at low concentration

To validate the applicability of PG-PB at environmentally relevant concentrations of PFOA, adsorption experiments were carried out at initial PFOA concentrations ranging from 0.01 to 2 mg/L. The results (Fig. 5a) indicate that PG-PB has excellent removal efficiency (96.4%) even at a PFOA concentration as low as 10 μg/L. As the initial PFOA concentration increased, the q_e value increased linearly. At an initial PFOA concentration of 2 mg/L, q_e reached 4.95 mg/g and the removal efficiency was 99.1%. The results indicate that the maximum adsorption capacity was not reached at low concentrations of PFOA, which suggests that changes in pH may not significantly affect PFOA removal efficiency at these concentrations. Thus, PG-PB appears to be a feasible option for removing PFOA within the environmentally relevant concentration range. However, considering that PG-PB has a high adsorption capacity for PFOA, and that high concentration of PFOA is needed in subsequent degradation processes, the pH effect, isotherms, kinetics and desorption experiments were investigated under a higher PFOA concentration level.

3.4.2. Effect of pH

The effect of pH on PFOA adsorption by PG-PB was studied with a contact time of 4 h; the results are given in Fig. 5b. The results show that the pH has a significant impact on PFOA adsorption by PG-PB. In general, PG-PB was able to adsorb more PFOA at lower pH. More than 89.2% (q_e = 446.1 mg/g) PFOA was removed at pH 2. At higher pH conditions, the adsorption performance significantly decreased, although it was still high. At an initial pH of 6, 7 and 8, the q_e values were reduced to 293.0, 258.0 and 259.4 mg/g, respectively. When the pH was adjusted to 11, only 30.8% (q_e = 154.2 mg/g) of the PFOA was removed from the water. The high PFOA removal efficiency at low pH could be attributed to the protonated amine groups under acidic conditions (Liu et al., 2018), which provided further binding sites in addition to the quaternary ammonium group. A similar trend was observed in a previous study related to sulfate adsorption by aminated peat (Gogoi et al., 2019). This also indicates that the hydroxide anion might compete with the PFOA anion for adsorption sites on PG-PB, which implies that NaOH can be used as a desorption solution for PG-PB regeneration. The pH values after adsorption were recorded and the pH was subjected to

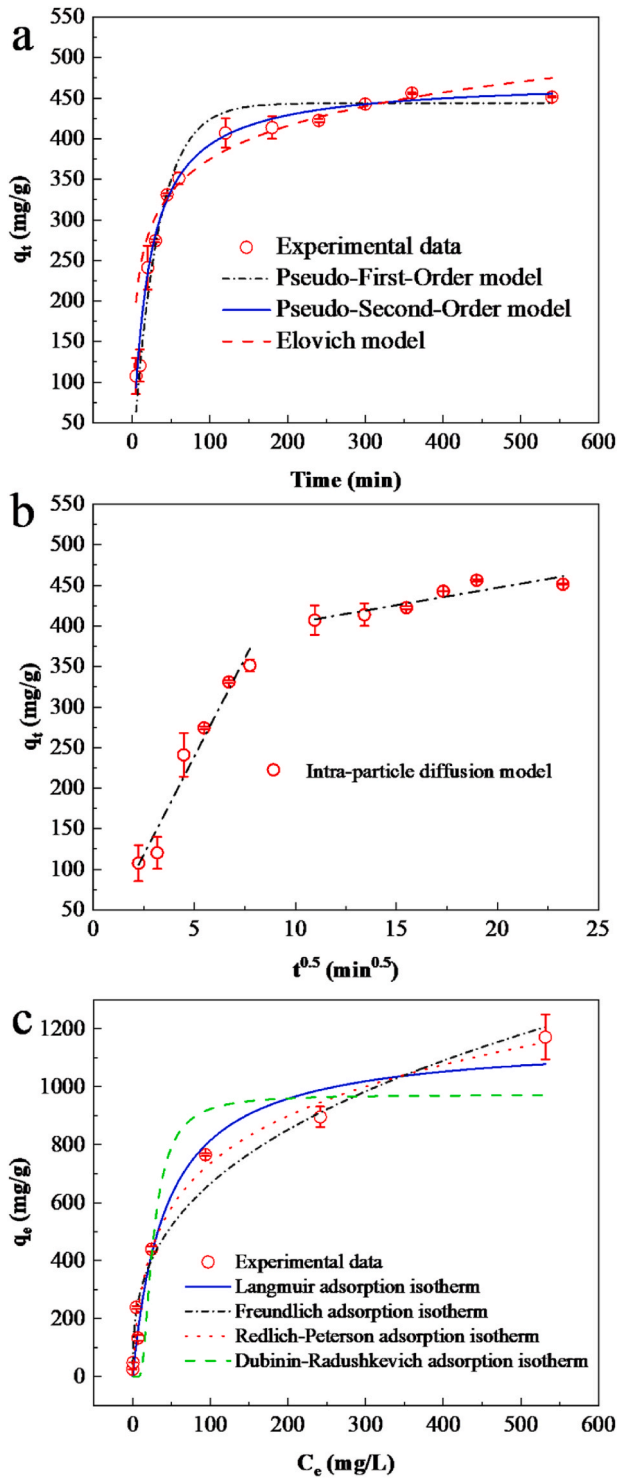

Fig. 6. a) Pseudo-first-order, pseudo-second-order, Elovich and b) intra-particle diffusion kinetics by a non-linear model and experimental kinetics for the sorption of PFOA onto PG-PB; c) Langmuir, Freundlich, Redlich-Peterson and Dubinin-Radushkevich isotherms obtained with non-linear equations and experimental data for the sorption of PFOA onto PG-PB (PFOA concentration in kinetics: 200 mg/L, PG-PB dosage: 0.4 g/L, pH = 3.3, contact time for isotherms = 24 h, T = 21 °C).

change during the adsorption experiment (Fig. 5b). In the experiments with an initial pH of below 7, the pH increased after adsorption, whereas in the experiments with an initial pH of above 7 a decrease in pH after adsorption was observed. This could be attributed to the equilibrium between the PG-PB surface and the aqueous medium during the adsorption process. It has been reported that the aqueous pKa of PFOA is in the range of −0.5 to 4.2 (Zango et al., 2023), and most likely between 0 and 1 (Rayne and Forest, 2010; Cheng et al., 2009). This means PFOA existed as deprotonated anions in this study.

Based on the results of the pH tests and the literature, the dominant mechanism responsible for PFOA adsorption is the electrostatic interaction between PFOA anions and quaternary ammonium groups on PG-PB. In addition, a large amount of amine groups on PG-PB are protonated at low pH values (Gogoi et al., 2019; Elwakeel, 2010), and the electrostatic attraction between cationic amine groups and PFOA anions further enhances the PFOA adsorption. Apart from electrostatic interaction, hydrophobic interaction most likely plays an important role in PFOA adsorption (Dixit et al., 2021). Studies have shown that PFOA and PFOS can form hemi-micelles on the surface of a sorbent even when the concentration is as low as 0.1%–1% critical micelle concentration (CMC) (CMC_{PFOA}: 15 696 mg/L, CMC_{PFOS}: 4573 mg/L) (Du et al., 2014; Baran et al., 2001; Johnson et al., 2007; Yu et al., 2009). For example, once the carboxyl head of PFOA had bonded to the positive surface, the hydrophobic tail of PFOA could aggregate and form a micelle bi-layer or hemi-micelle with other PFOA molecules (Liu et al., 2018; Chen et al., 2017), which further increased the PFOA uptake capacity. In summary, the main adsorption mechanisms that contributed to PFOA adsorption on PG-PB were ion exchange, electrostatic attraction and hydrophobic interaction.

3.4.3. Adsorption kinetics and isotherms

The effect of contact time on PFOA adsorption by PG-PB is presented in Fig. 6a and b. The adsorption of PFOA needs a rather long time (6 h) to reach equilibrium. However, 81.4% of the PFOA was rapidly removed from the water within 2 h, resulting in an adsorption capacity of ≈407 mg/g. During this period, the cationic sites (quaternary ammonium groups and protonated amine groups) were quickly filled with PFOA anions. Then the removal efficiency was gradually increased and finally reached equilibrium with an adsorption capacity of ≈456 mg/g (91.3% of the PFOA was removed) at 6 h, after which it remained >450 mg/g throughout the tests with longer contact times (6–9 h).

The kinetic experimental data of PFOA adsorption were fitted into non-linear PFO, PSO, intra-particle diffusion, Boyd and Elovich equations. The obtained parameters of each model are given in Table S2. Among these models, the PSO model provided the best fit to the experimental data due to its highest correlation coefficient ($R^2 = 0.988$), lowest chi-square value ($\chi^2 = 11.7$) and good prediction of q_e (472.6 mg/g) compared to the q_{exp} (456.0 mg/g). This indicates that the PSO model is adequate to describe the PFOA adsorption process by PG-PB, whereas the intra-particle diffusion and Elovich models have a low R^2 (0.748 and 0.917) and high χ^2 (289.0 and 111.8), which means they are not suitable for evaluating the PFOA adsorption process. The Elovich model is typically used to describe the chemisorption process (McLintock, 1967). The low R^2 and high χ^2 values indicated that the PFOA adsorption mechanisms were not governed fully by chemisorption. The intra-particle diffusion model is used for identifying the reaction pathways and adsorption mechanisms. The plot of q_t against $t^{0.5}$ gives two linear regions (Fig. 6b), referring to a multistep mechanism although the fitting to the experimental data is rather poor. The Boyd model was employed to determine the rate-limiting step by analysing the plot of B_t versus time (t). If the plot is linear and passes through the origin, intra-particle diffusion is the rate-limiting step. Otherwise, film diffusion is likely to be the rate-limiting step. The results given in the supporting information (Fig. S8) showed that the plot is not linear and did not pass through the origin. This suggests that adsorption was probably controlled by film diffusion.

The adsorption isotherm experiments were performed with an initial PFOA concentration from 10 to 1000 mg/L. The non-linear Langmuir, Freundlich, Redlich-Peterson and Dubinin-Radushkevich equations were used to fit the experimental data of the PFOA adsorption isotherm.

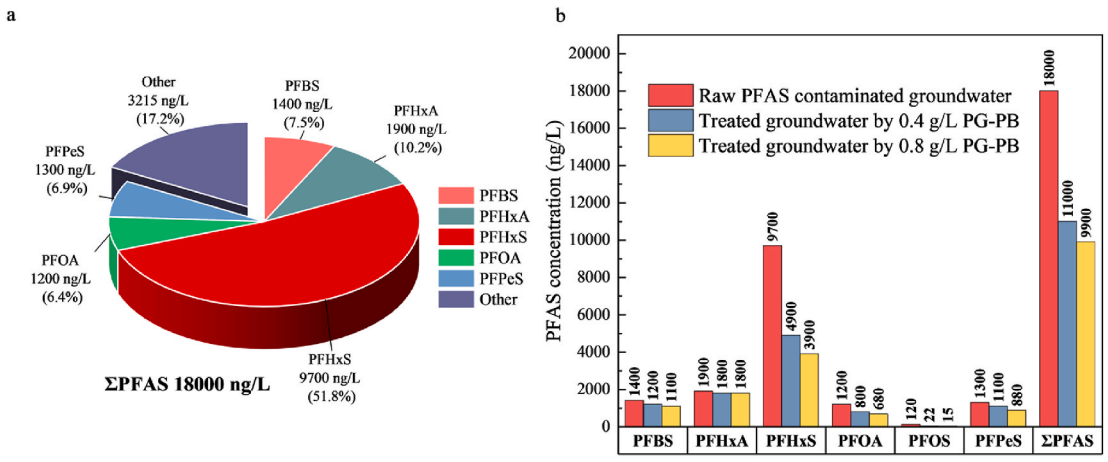

Fig. 7. a) Concentrations and proportion of the main PFAS in the contaminated groundwater; b) adsorption results of the 6 main PFAS by PG-PB (PG-PB dosage: 0.4 and 0.8 g/L, adsorption time: 24 h, temperature: 21 °C, pH = 7).

Table 2
Distribution coefficients (K_d) of the main PFAS in the contaminated groundwater.

PFAS species	K_d (L/g), 0.4 g/L of PG-PB	K_d (L/g), 0.8 g/L of PG-PB
PFBS	0.417	0.341
PFHxA	0.139	0.069
PFHxS	2.449	1.859
PFOA	1.250	0.956
PFOS	11.136	8.750
PFPeS	0.202	0.146

The related parameters of the two models are shown in Table S3 and the fitting curves are given in Fig. 6c. Of the four models, the Redlich-Peterson model has the highest R^2 (0.986) although the χ^2 (270.9) of the model was high, which means the fitting has some defects. Compared with the Redlich-Peterson model, the Freundlich model gives a better fit as it has a high R^2 (0.973) and lower χ^2 (122.4), indicating the multilayer adsorption of PFOA on the heterogenous surface of the PG-PB (Tran et al., 2017). As shown in Fig. 6c, the maximum PFOA adsorption capacity of PG-PB reached 1171.3 mg/g with the initial PFOA concentration of 1 g/L. The high adsorption capacity could be attributed to the large number of active binding sites of PG-PB and the unique composition of PFOA. Unlike common inorganic anions, PFOA anions have a long tail with a hydrophobic property, which makes it easy to form micelles and hemi-micelles with other PFOA anions (Du et al., 2014). The column adsorption results and discussion are given in supporting information Section S2. The high adsorption capacity and fast kinetics of PG-PB make it an excellent sorbent for PFAS contamination.

In other studies related to PFOA adsorption, powdered activated carbons achieved capacities of 175–524 mg/g (Du et al., 2014), granular activated carbons achieved 112–161 mg/g (Du et al., 2014), and AER 331–1436 mg/g (Gagliano et al., 2020). Thus, the capacity of PG-PB (1173 mg/g) is close to the maximum capacity of AER, while it is significantly higher when compared to the non-modified ACs. The high adsorption efficiency is attributed to the numerous amine groups present on the surface of the materials, which facilitate electrostatic attraction between the protonated amine groups and anionic PFOA (Du et al., 2014). While commercial resins share many of the same characteristics as PG-PB, one notable advantage of PG-PB is its lower cost compared with commercial resins (Du et al., 2014).

3.5. Groundwater treatment

It is essential to investigate the effectiveness of PG-PB in treating real PFAS-contaminated water when considering a practical application. The concentrations and proportions of the first five main PFAS contaminants in the groundwater are given in Fig. 7a. The concentration of perfluorohexanesulfonic acid (PFHxS) in the groundwater was detected to be 9700 ng/L, which accounted for 51.8% of the total 28 PFAS. The results of all the adsorption experiments are given in Fig. 7b and full results can be found in Table S5. The distribution coefficients K_d (equations are given in Section S1) (US EPA, 2022) of the main PFAS were calculated to estimate their distribution between adsorbent and water (Table 2). In general, the total concentration of the 28 PFAS was greatly reduced, from 18 000 ng/L to 11 000 ng/L and 9900 ng/L by 0.4 g/L and 0.8 g/L dosages of PG-PB, respectively. The PG-PB showed high removal efficiency for PFHxS and PFOA in that 59.8% PFHxS (K_d: 1.859 L/g) and 43.3% PFOA (K_d: 0.956 L/g) were removed by 0.8 g/L PG-PB. Also, despite the low PFOS concentration (120 ng/L) in the groundwater, 87.5% of the PFOS was removed by 0.8 g/L PG-PB with a high K_d value of 8.750 L/g. This finding suggests that PG-PB is effective in binding PFOS, even at low concentrations, and could potentially prevent the spread of PFOS to the surrounding environment. However, compared to PFHxS, PFOA and PFOS, other short-chain PFAS, such as perfluorobutanesulfonic acid (PFBS), perfluorohexanoic acid (PFHxA) and perfluoropentanesulfonic acid (PFPeS), were hardly removed at all by PG-PB. The possible reason for this is that short-chain PFAS have much lower hydrophobicity than long-chain PFAS, which results in lower adsorption efficiency. Nevertheless, as the PG-PB was validated to be highly efficient for PFAS removal at low concentration levels of PFAS, the usage of PG-PB for PFAS-contaminated groundwater treatment is feasible.

3.6. Regeneration studies on PG-PB

To test the reusability of PG-PB, several different desorption eluents were preliminarily selected for regeneration experiments and the adsorption after each regeneration step was also examined (Fig. 8a and b). In Fig. 8a, it is clear that water and NaCl solution (5% and 10%) show very poor desorption efficiency for the used PG-PB (up to 1.7% PFOA recovery by 5% NaCl). In contrast, NaOH solution (1% and 2%) and 100% MeOH exhibited acceptable desorption efficiency (up to 59.1% with 1% NaOH). Moreover, the presence of MeOH in the NaOH solution enhances the desorption. The mixture of NaOH and MeOH solution was effective for PFOA desorption (up to 92.5% PFOA recovery by 50% MeOH + 0.2% NaOH). However, it can be seen in Fig. 8b that the adsorption capacity of regenerated PG-PB by NaOH and MeOH + NaOH mixture decreased slightly. One possible explanation is that very alkaline conditions could dissolve cellulose from the surface of the PG-PB (Kim et al., 2016; Zhong et al., 2017), which would lead to the loss of

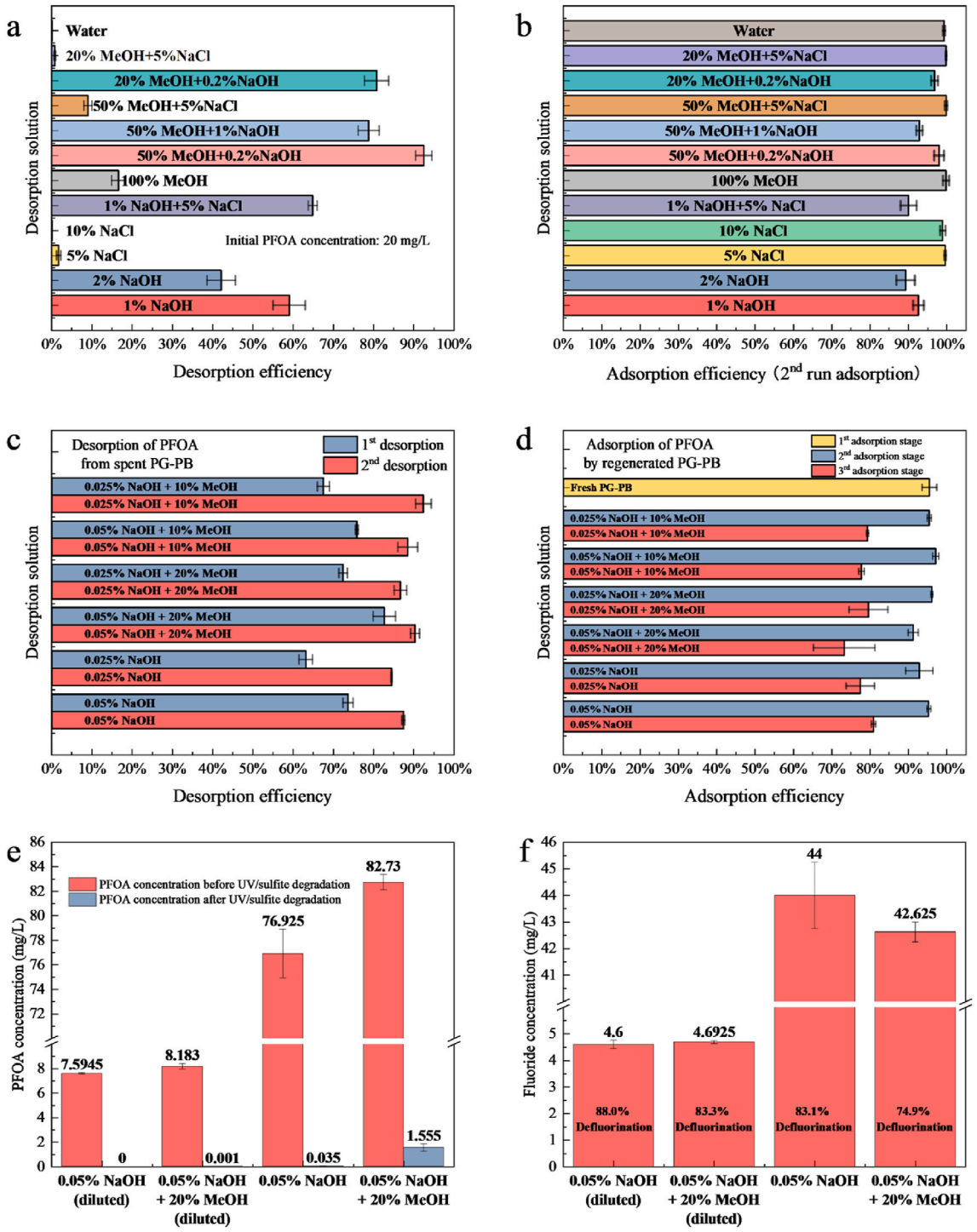

Fig. 8. a) PFOA desorption by different desorption solutions; b) PFOA adsorption by regenerated PG-PB. c) desorption of PFOA from spent PG-PB and d) adsorption of PFOA by regenerated PG-PB; photocatalytic degradation of PFOA desorption solution in the UV/sulfite system: e) PFOA degradation; f) defluorination (PFOA initial concentration: 20 mg/L in a and b, 100 mg/L in c-f, desorption time: 4 h, adsorption time: 24 h, PG-PB dosage: 0.4 g/L, no pH adjustment, degradation time: 24 h, sulfite dosage: 10 mM, T = 21 °C).

adsorption capacity. However, it must be borne in mind that the PG-PB was modified in alkaline conditions (2 g/L of NaOH (0.2%)). Therefore, it was considered feasible to use alkaline conditions, i.e. at least 0.2% NaOH, for PG-PB regeneration. In the following regeneration experiments, the NaOH solution as well as the mixture of MeOH and NaOH solution were used as desorption solutions and the percentage of NaOH was reduced to prevent a loss of adsorption capacity.

According to the preliminary tests, NaOH solution (0.05% and 0.025%) and a mixture of NaOH + MeOH were chosen as the desorption eluent for further desorption tests, and the initial PFOA concentration was increased to 100 mg/L. The results showed that the 1st desorption efficiency with 0.05% NaOH (73.7%) was more effective than with 0.025% NaOH (63.2%). Also, the presence of MeOH in the NaOH solution enhanced the desorption efficiency. In addition, the presence of 10% and 20% MeOH in 0.025% NaOH solution increased the desorption efficiency to 67.6% and 72.5% (Fig. 8c), respectively. For the desorption

eluents containing 0.05% NaOH + 10% MeOH and 0.05% NaOH + 20% MeOH, the desorption efficiency increased to 75.9% and 82.7%, respectively. Similar results were observed in the 2nd desorption experiments. It is likely that the presence of methanol weakened the hydrophobic interaction of PFOA (Zaggia et al., 2016), which helped to release more PFOA from the sorbent into the water and slightly increased the desorption efficiency. Therefore, the addition of MeOH to NaOH solution could be a feasible method to improve the desorption performance in practical applications. However, the 2nd desorption was able to release more PFOA from the used PG-PB compared to the 1st desorption. A possible explanation is that PG-PB has different active sites on its surface. Some active sites such as the quaternary ammonium group could bind PFOA tightly and be difficult to desorb with NaOH, whereas other sites like protonated amine groups could be easily recovered by NaOH and release PFOA into the water. The mechanism of desorption and UV/sulfite degradation is illustrated in Fig. S10.

Fresh PG-PB was able to remove 95% of the PFOA from the water. In the 2nd adsorption stage (Fig. 8d), the regenerated PG-PB was still able to remove 93–97% of the PFOA despite the incomplete desorption. However, a further decrease in the adsorption efficiency was observed in the 3rd adsorption stage. One possible explanation is that the surface structure and functional groups changed during the long contact time with NaOH due to the dissolution of hemicellulose and lignin (Kim et al., 2016; Mwaikambo and Ansell, 2002). Thus, it is better to accept partial regeneration than to use too strong conditions for regeneration. Nevertheless, it was confirmed that the reuse of PG-PB is possible, and NaOH as well as a mixture of NaOH and MeOH can be used for PG-PB regeneration.

3.7. Photocatalytic degradation of PFOA from desorption effluent

The desorption effluent was subjected to photocatalytic degradation (UV/sulfite system). The desorption solutions were 0.05% NaOH and 0.05% NaOH + 20% MeOH as their desorption efficiencies were the highest according to the results (Fig. 8c). The photocatalytic degradation results are given in Fig. 8e and f.

The average concentration of PFOA in the diluted (10-fold) desorption effluents was 7.60 mg/L (0.05% NaOH) and 8.18 mg/L (0.05% NaOH + 20% MeOH), and the pH values were around 10.9. In the non-diluted desorption effluents, the PFOA concentration was 76.93 mg/L (0.05% NaOH) and 82.73 mg/L (0.05% NaOH + 20% MeOH), and the pH values were around 11.5. The results (Fig. 8e) showed that almost all of the PFOA was removed from the diluted desorption effluents after 24 h of degradation. However, 1.56 mg/L of PFOA was detected in the non-diluted 0.05% NaOH + 20% MeOH effluent. The defluorination efficiency is known as a key factor when evaluating PFAS degradation performance. As the initial PFOA concentrations differed, the defluorination efficiency was calculated to evaluate the degradation performance (Fig. 8f). The average defluorination efficiencies were 88.0% and 83.3% in the diluted 0.05% NaOH and 0.05% NaOH + 20% MeOH, respectively. In the non-diluted desorption effluents, the defluorination efficiencies were 83.1% and 74.9% in 0.05% NaOH and 0.05% NaOH + 20% MeOH, respectively. The above results indicate that a high concentration of MeOH may have an adverse effect on PFOA degradation in a UV/sulfite system. This may be because the MeOH was able to react with hydrated electrons and hence reduced the defluorination efficiency (Bolton et al., 1976). However, a high defluorination efficiency (74.9%) could still be achieved even in the presence of 20% MeOH. Therefore, in practical applications, the addition of MeOH could be considered as it could slightly increase the desorption efficiency while sacrificing some defluorination performance. One possible solution to keep the advantages and eliminate the disadvantages is to recycle the MeOH by evaporation before UV/sulfite degradation (Boyer et al., 2021b).

4. Conclusions and perspectives

The contamination of water by PFAS usually involves several challenges, such as low concentration, wide distribution, large volume and a long decomposition period, which makes it difficult to achieve PFAS mineralization in contaminated water using a single treatment method. Therefore, to overcome these challenges, a combined adsorption/desorption and UV/sulfite degradation process for PFOA elimination was investigated and optimized in this study. A novel biosorbent was successfully synthesized and applied for PFOA adsorption and desorption. XPS, FTIR and SEM- EDS analyses revealed that amine groups and quaternary ammonium groups were the main functional groups grafted onto the PB surface, and both the amine and quaternary ammonium groups contributed to the high PFOA adsorption capacity. The developed PG-PB is highly efficient in terms of PFOA uptake from water at low or natural pH values, exhibiting great potential for the treatment of PFOA-contaminated water. The adsorption/desorption results show that PG-PB has a high adsorption capacity for PFOA and that it can be regenerated and reused. The photo-reductive degradation of PFOA in the desorption effluent by a UV/sulfite system reached high levels of degradation and defluorination efficiency, indicating that the combination of adsorption/desorption and a UV/sulfite process is a feasible method for PFOA removal.

Credit author statement

Zhongfei Ren: Conceptualization, Methodology, Data curation, Writing- Original draft preparation, Writing- Reviewing and Editing, Software, Formal analysis, Visualization, Investigation, Validation. **Ulrich Bergmann:** Methodology, Data curation, Reviewing and Editing, **Jean Noel Uwayezu:** Resources, Reviewing and Editing, **Ivan Carabante:** Funding acquisition, Resources, Reviewing and Editing. **Jurate Kumpiene:** Funding acquisition, Methodology, Resources, Reviewing and Editing. **Tore Lejon:** Funding acquisition, Methodology, Resources, Reviewing and Editing. **Tiina Leiviskä:** Supervision, Funding acquisition, Conceptualization, Methodology, Resources, Writing- Reviewing and Editing.

Declaration of competing interest

The authors declare that they have no known competing financial interests or personal relationships that could have appeared to influence the work reported in this paper.

Data availability

Data will be made available on request.

Acknowledgements

The research was conducted as part of the Less-PFAS project “Sustainable management of PFAS-contaminated materials (ID: 20202462)”, funded by the European Union program Interreg Nord 2019–2022 and the Regional Council of Lapland, Norrbotten County Council and Troms og Finnmark County Municipality.

Appendix A. Supplementary data

Supplementary data to this article can be found online at https://doi.org/10.1016/j.envres.2023.115930.

References

Baran, J.R., 2001. Fluorinated surfactants and repellents. New York. In: Kissa, Erik, Wilmington, D.E., Marcel Dekker (Eds.), Revised and Expanded Surfactant Science Series, second ed., vol. 97. https://doi.org/10.1021/ja015260a xiv + 616 pp. $195.00. ISBN 0-8247-0472-X., J. Am. Chem. Soc. 123 (2001) 8882–8882.

Beale, D.J., Hillyer, K., Nilsson, S., Limpus, D., Bose, U., Broadbent, J.A., Vardy, S., 2022. Bioaccumulation and metabolic response of PFAS mixtures in wild-caught freshwater turtles (Emydura macquarii macquarii) using omics-based ecosurveillance techniques. Sci. Total Environ. 806, 151264 https://doi.org/10.1016/j.scitotenv.2021.151264.

Bentel, M.J., Yu, Y., Xu, L., Li, Z., Wong, B.M., Men, Y., Liu, J., 2019. Defluorination of per- and polyfluoroalkyl substances (PFASs) with hydrated electrons: structural dependence and implications to PFAS remediation and management. Environ. Sci. Technol. 53, 3718–3728. https://doi.org/10.1021/acs.est.8b06648.

Blanchard, G., Maunaye, M., Martin, G., 1984. Removal of heavy metals from waters by means of natural zeolites. Water Res. 18, 1501–1507. https://doi.org/10.1016/0043-1354(84)90124-6.

Bolton, G.L., Robinson, M.G., Freeman, G.R., 1976. Reaction rates of electrons in liquid methanol and ethanol: effects of pressure. Can. J. Chem. 54, 1177–1188. https://doi.org/10.1139/v76-167.

Boyd, G.E., Adamson, A.W., Myers Jr., L.S., 1947. The exchange adsorption of ions from aqueous solutions by organic zeolites. II. Kinetics1. J. Am. Chem. Soc. 69, 2836–2848. https://doi.org/10.1021/ja01203a066.

Boyer, T.H., Fang, Y., Ellis, A., Dietz, R., Choi, Y.J., Schaefer, C.E., Higgins, C.P., Strathmann, T.J., 2021a. Anion exchange resin removal of per- and polyfluoroalkyl substances (PFAS) from impacted water: a critical review. Water Res. 200, 117244 https://doi.org/10.1016/j.watres.2021.117244.

Boyer, T.H., Ellis, A., Fang, Y., Schaefer, C.E., Higgins, C.P., Strathmann, T.J., 2021b. Life cycle environmental impacts of regeneration options for anion exchange resin remediation of PFAS impacted water. Water Res. 207, 117798 https://doi.org/10.1016/j.watres.2021.117798.

Burns, D.J., Stevenson, P., Murphy, P.J.C., 2021. PFAS removal from groundwaters using Surface-Active Foam Fractionation. Remed. J. 31, 19–33. https://doi.org/10.1002/rem.21694.

Cao, W., Wang, Z., Zeng, Q., Shen, C., 2016. 13C NMR and XPS characterization of anion adsorbent with quaternary ammonium groups prepared from rice straw, corn stalk and sugarcane bagasse. Appl. Surf. Sci. 389, 404–410. https://doi.org/10.1016/j.apsusc.2016.07.095.

Chen, J., Zhang, P., 2006. Photodegradation of perfluorooctanoic acid in water under irradiation of 254 nm and 185 nm light by use of persulfate. Water Sci. Technol. 54, 317–325. https://doi.org/10.2166/wst.2006.731.

Chen, W., Zhang, X., Mamadiev, M., Wang, Z., 2017. Sorption of perfluorooctane sulfonate and perfluorooctanoate on polyacrylonitrile fiber-derived activated carbon fibers: in comparison with activated carbon. RSC Adv. 7, 927–938. https://doi.org/10.1039/C6RA25230C.

Cheng, J., Psillakis, E., Hoffmann, M.R., Colussi, A.J., 2009. Acid dissociation versus molecular association of perfluoroalkyl oxoacids: environmental implications. J. Phys. Chem. 113, 8152–8156. https://doi.org/10.1021/jp9051352.

Chu, K.H., 2010. Fixed bed sorption: setting the record straight on the Bohart–Adams and Thomas models. J. Hazard Mater. 177, 1006–1012. https://doi.org/10.1016/j.jhazmat.2010.01.019.

Deng, S., Niu, L., Bei, Y., Wang, B., Huang, J., Yu, G., 2013. Adsorption of perfluorinated compounds on aminated rice husk prepared by atom transfer radical polymerization. Chemosphere 91, 124–130. https://doi.org/10.1016/j.chemosphere.2012.11.015.

DiStefano, R., Feliciano, T., Mimna, R.A., Redding, A.M., Matthis, J., 2022. Thermal destruction of PFAS during full-scale reactivation of PFAS-laden granular activated carbon. Remed. J. 32, 231–238. https://doi.org/10.1002/rem.21735.

Dixit, F., Barbeau, B., Mostafavi, S.G., Mohseni, M., 2020. Removal of legacy PFAS and other fluorotelomers: optimized regeneration strategies in DOM-rich waters. Water Res. 183, 116098 https://doi.org/10.1016/j.watres.2020.116098.

Dixit, F., Dutta, R., Barbeau, B., Berube, P., Mohseni, M., 2021. PFAS removal by ion exchange resins: a review. Chemosphere 272, 129777. https://doi.org/10.1016/j.chemosphere.2021.129777.

Du, Z., Deng, S., Bei, Y., Huang, Q., Wang, B., Huang, J., Yu, G., 2014. Adsorption behavior and mechanism of perfluorinated compounds on various adsorbents—a review. J. Hazard Mater. 274, 443–454. https://doi.org/10.1016/j.jhazmat.2014.04.038.

Dubinin, M., 1947. The Equation of the Characteristic Curve of Activated Charcoal, pp. 327–329. https://cir.nii.ac.jp/crid/1573950400604554624.

Elwakeel, K.Z., 2010. Removal of Cr(VI) from alkaline aqueous solutions using chemically modified magnetic chitosan resins. Desalination 250, 105–112. https://doi.org/10.1016/j.desal.2009.02.063.

Fleming, I., Williams, D., 2019. Infrared and Raman spectra. In: Fleming, I., Williams, D. (Eds.), Spectrosc. Methods Org. Chem. Springer International Publishing, Cham, pp. 85–121. https://doi.org/10.1007/978-3-030-18252-6_3.

Freundlich, H., 1907.. Über die adsorption in lösungen. Z. Phys. Chem. 57, 385–470. https://link.springer.com/article/10.1007/BF01466557.

Gagliano, E., Sgroi, M., Falciglia, P.P., Vagliasindi, F.G.A., Roccaro, P., 2020. Removal of poly- and perfluoroalkyl substances (PFAS) from water by adsorption: role of PFAS chain length, effect of organic matter and challenges in adsorbent regeneration. Water Res. 171, 115381 https://doi.org/10.1016/j.watres.2019.115381.

Ghisi, R., Vamerali, T., Manzetti, S., 2019. Accumulation of perfluorinated alkyl substances (PFAS) in agricultural plants: a review. Environ. Res. 169, 326–341. https://doi.org/10.1016/j.envres.2018.10.023.

Gogoi, H., Leiviskä, T., Rämö, J., Tanskanen, J., 2019. Production of aminated peat from branched polyethylenimine and glycidyltrimethylammonium chloride for sulphate removal from mining water. Environ. Res. 175, 323–334. https://doi.org/10.1016/j.envres.2019.05.022.

Guo, C., Zhang, C., Sun, Z., Zhao, X., Zhou, Q., Hoffmann, M.R., 2019. Synergistic impact of humic acid on the photo-reductive decomposition of perfluorooctanoic acid. Chem. Eng. J. 360, 1101–1110. https://doi.org/10.1016/j.cej.2018.10.204.

Helmer, R.W., Reeves, D.M., Cassidy, D.P., 2022. Per- and Polyfluorinated Alkyl Substances (PFAS) cycling within Michigan: contaminated sites, landfills and wastewater treatment plants. Water Res. 210, 117983 https://doi.org/10.1016/j.watres.2021.117983.

Herbert, H.L., 1960. Infrared spectra of lignin and related compounds. II. Conifer lignin and model Compounds1,2. J. Org. Chem. 25, 405–413. https://doi.org/10.1021/jo01073a026.

Jian, J.-M., Chen, D., Han, F.-J., Guo, Y., Zeng, L., Lu, X., Wang, F., 2018. A short review on human exposure to and tissue distribution of per- and polyfluoroalkyl substances (PFASs). Sci. Total Environ. 636, 1058–1069. https://doi.org/10.1016/j.scitotenv.2018.04.380.

Johnson, R.L., Anschutz, A.J., Smolen, J.M., Simcik, M.F., Penn, R.L., 2007. The adsorption of perfluorooctane sulfonate onto sand, clay, and iron oxide surfaces. J. Chem. Eng. Data 52, 1165–1170. https://doi.org/10.1021/je060285g.

Kim, J.S., Lee, Y.Y., Kim, T.H., 2016. A review on alkaline pretreatment technology for bioconversion of lignocellulosic biomass. Bioresour. Technol. 199, 42–48. https://doi.org/10.1016/j.biortech.2015.08.085.

Lagergren, S.K., 1898. About the theory of so-called adsorption of soluble substances. Sven Vetenskapsakad Handingarl 24, 1–39. https://cir.nii.ac.jp/crid/1570009750361875328.

Langmuir, I., 1918. The adsorption of gases on plane surfaces of glass, mica and platinum. J. Am. Chem. Soc. 40, 1361–1403. https://doi.org/10.1021/ja02242a004.

Lee, T., Speth, T.F., Nadagouda, M.N., 2022. High-pressure membrane filtration processes for separation of Per- and polyfluoroalkyl substances (PFAS). Chem. Eng. J. 431, 134023 https://doi.org/10.1016/j.cej.2021.134023.

Li, X., Chen, S., Fan, X., Quan, X., Tan, F., Zhang, Y., Gao, J., 2015. Adsorption of ciprofloxacin, bisphenol and 2-chlorophenol on electrospun carbon nanofibers: in comparison with powder activated carbon. J. Colloid Interface Sci. 447, 120–127. https://doi.org/10.1016/j.jcis.2015.01.042.

Li, F., Duan, J., Tian, S., Ji, H., Zhu, Y., Wei, Z., Zhao, D., 2020. Short-chain per- and polyfluoroalkyl substances in aquatic systems: occurrence, impacts and treatment. Chem. Eng. J. 380, 122506 https://doi.org/10.1016/j.cej.2019.122506.

Lin, H., Wang, Y., Niu, J., Yue, Z., Huang, Q., 2015. Efficient sorption and removal of perfluoroalkyl acids (PFAAs) from aqueous solution by metal hydroxides generated in situ by electrocoagulation. Environ. Sci. Technol. 49, 10562–10569. https://doi.org/10.1021/acs.est.5b02092.

Liu, L., Li, D., Li, C., Ji, R., Tian, X., 2018. Metal nanoparticles by doping carbon nanotubes improved the sorption of perfluorooctanoic acid. J. Hazard Mater. 351, 206–214. https://doi.org/10.1016/j.jhazmat.2018.03.001.

Lu, D., Sha, S., Luo, J., Huang, Z., Zhang Jackie, X., 2020. Treatment train approaches for the remediation of per- and polyfluoroalkyl substances (PFAS): a critical review. J. Hazard Mater. 386, 121963 https://doi.org/10.1016/j.jhazmat.2019.121963.

Macheka-Tendenguwo, L.R., Olowoyo, J.O., Mugivhisa, L.L., Abafe, O.A., 2018. Per- and polyfluoroalkyl substances in human breast milk and current analytical methods. Environ. Sci. Pollut. Res. 25, 36064–36086. https://doi.org/10.1007/s11356-018-3483-z.

McLintock, I.S., 1967. The Elovich equation in chemisorption kinetics. Nature 216, 1204–1205. https://doi.org/10.1038/2161204a0.

Mwaikambo, L.Y., Ansell, M.P., 2002. Chemical modification of hemp, sisal, jute, and kapok fibers by alkalization. J. Appl. Polym. Sci. 84, 2222–2234. https://doi.org/10.1002/app.10460.

Qian, Y., Guo, X., Zhang, Y., Peng, Y., Sun, P., Huang, C.-H., Niu, J., Zhou, X., Crittenden, J.C., 2016. Perfluorooctanoic acid degradation using UV–persulfate process: modeling of the degradation and chlorate formation. Environ. Sci. Technol. 50, 772–781. https://doi.org/10.1021/acs.est.5b03715.

Rahman, M.F., Peldszus, S., Anderson, W.B., 2014. Behaviour and fate of perfluoroalkyl and polyfluoroalkyl substances (PFASs) in drinking water treatment: a review. Water Res. 50, 318–340. https://doi.org/10.1016/j.watres.2013.10.045.

Rayne, S., Forest, K., 2010. Theoretical studies on the pKa values of perfluoroalkyl carboxylic acids. J. Mol. Struct. THEOCHEM. 949, 60–69. https://doi.org/10.1016/j.theochem.2010.03.003.

Redlich, O., Peterson, D.L., 1959. A useful adsorption isotherm. J. Phys. Chem. 63 https://doi.org/10.1021/j150576a611, 1024–1024.

Ren, Z., Xu, X., Gao, B., Yue, Q., Song, W., 2015. Integration of adsorption and direct bio-reduction of perchlorate on surface of cotton stalk based resin. J. Colloid Interface Sci. 459, 127–135. https://doi.org/10.1016/j.jcis.2015.08.016.

Ren, Z., Xu, X., Qi, S., Li, Y., Gao, B., song, W., Jiang, P., 2017. Uptake of phosphate and Cr(VI) by amine-functionalized Chinese reed: considering the computations and characteristics analysis. J. Taiwan Inst. Chem. Eng. 72, 85–94. https://doi.org/10.1016/j.jtice.2017.01.007.

Ren, Z., Bergmann, U., Leiviskä, T., 2021. Reductive degradation of perfluorooctanoic acid in complex water matrices by using the UV/sulfite process. Water Res. 205, 117676 https://doi.org/10.1016/j.watres.2021.117676.

Song, Z., Tang, H., Wang, N., Zhu, L., 2013. Reductive defluorination of perfluorooctanoic acid by hydrated electrons in a sulfite-mediated UV photochemical system. J. Hazard Mater. 262, 332–338. https://doi.org/10.1016/j.jhazmat.2013.08.059.

Sowmya, A., Meenakshi, S., 2014. A novel quaternized chitosan–melamine–glutaraldehyde resin for the removal of nitrate and phosphate anions. Int. J. Biol. Macromol. 64, 224–232. https://doi.org/10.1016/j.ijbiomac.2013.11.036.

Stockholm Convention, 2019. https://chm.pops.int/TheConvention/Overview/TextoftheConvention/tabid/2232/Default.aspx.

Su, Y., Lu, M., Su, R., Zhou, W., Xu, X., Li, Q., 2022. A 3D MIL-101@rGO composite as catalyst for efficient conversion of straw cellulose into valuable organic acid. Chin. Chem. Lett. 33, 2573–2578. https://doi.org/10.1016/j.cclet.2021.08.078.

Sunderland, E.M., Hu, X.C., Dassuncao, C., Tokranov, A.K., Wagner, C.C., Allen, J.G., 2019. A review of the pathways of human exposure to poly- and perfluoroalkyl substances (PFASs) and present understanding of health effects. J. Expo. Sci. Environ. Epidemiol. 29, 131–147. https://doi.org/10.1038/s41370-018-0094-1.

Tran, H.N., You, S.-J., Hosseini-Bandegharaei, A., Chao, H.-P., 2017. Mistakes and inconsistencies regarding adsorption of contaminants from aqueous solutions: a critical review. Water Res. 120, 88–116. https://doi.org/10.1016/j.watres.2017.04.014.

US EPA, 2022. Understanding Variation in Partition Coefficient, Kd, Values. https://www.epa.gov/radiation/understanding-variation-partition-coefficient-kd-values.

US EPA, 2022. Drinking Water Health Advisories for PFOA and PFOS. https://www.epa.gov/sdwa/drinking-water-health-advisories-pfoa-and-pfos.

Uwayezu, J.N., Carabante, I., Lejon, T., van Hees, P., Karlsson, P., Hollman, P., Kumpiene, J., 2021. Electrochemical degradation of per- and poly-fluoroalkyl substances using boron-doped diamond electrodes. J. Environ. Manag. 290, 112573 https://doi.org/10.1016/j.jenvman.2021.112573.

Vu, C.T., Wu, T., 2020. Adsorption of short-chain perfluoroalkyl acids (PFAAs) from water/wastewater. Environ. Sci. Water Res. Technol. 6, 2958–2972. https://doi.org/10.1039/D0EW00468E.

Weber, W.J., Morris, J.C., 1963. Kinetics of adsorption on carbon from solution. J. Sanit. Eng. Div. 89, 31–59. https://doi.org/10.1061/JSEDAI.0000430.

Xu, C., Chen, H., Jiang, F., 2015. Adsorption of perflourooctane sulfonate (PFOS) and perfluorooctanoate (PFOA) on polyaniline nanotubes. Colloids Surf. A Physicochem. Eng. Asp. 479, 60–67. https://doi.org/10.1016/j.colsurfa.2015.03.045.

Xu, B., Liu, S., Zhou, J.L., Zheng, C., Weifeng, J., Chen, B., Zhang, T., Qiu, W., 2021. PFAS and their substitutes in groundwater: occurrence, transformation and remediation. J. Hazard Mater. 412, 125159 https://doi.org/10.1016/j.jhazmat.2021.125159.

Yu, Q., Zhang, R., Deng, S., Huang, J., Yu, G., 2009. Sorption of perfluorooctane sulfonate and perfluorooctanoate on activated carbons and resin: kinetic and isotherm study. Water Res. 43, 1150–1158. https://doi.org/10.1016/j.watres.2008.12.001.

Yuan, J., Mortazavian, S., Passeport, E., Hofmann, R., 2022. Evaluating perfluorooctanoic acid (PFOA) and perfluorooctanesulfonic acid (PFOS) removal across granular activated carbon (GAC) filter-adsorbers in drinking water treatment plants. Sci. Total Environ. 838, 156406 https://doi.org/10.1016/j.scitotenv.2022.156406.

Zaggia, A., Conte, L., Falletti, L., Fant, M., Chiorboli, A., 2016. Use of strong anion exchange resins for the removal of perfluoroalkylated substances from contaminated drinking water in batch and continuous pilot plants. Water Res. 91, 137–146. https://doi.org/10.1016/j.watres.2015.12.039.

Zango, Z.U., Khoo, K.S., Garba, A., Kadir, H.A., Usman, F., Zango, M.U., Da Oh, W., Lim, J.W., 2023. A review on superior advanced oxidation and photocatalytic degradation techniques for perfluorooctanoic acid (PFOA) elimination from wastewater. Environ. Res. 221, 115326 https://doi.org/10.1016/j.envres.2023.115326.

Zhong, C., Cheng, F., Zhu, Y., Gao, Z., Jia, H., Wei, P., 2017. Dissolution mechanism of cellulose in quaternary ammonium hydroxide: revisiting through molecular interactions. Carbohydr. Polym. 174, 400–408. https://doi.org/10.1016/j.carbpol.2017.06.078.

Zou, X., Zhao, X., Ye, L., 2015. Synthesis of cationic chitosan hydrogel with long chain alkyl and its controlled glucose-responsive drug delivery behavior. RSC Adv. 5, 96230–96241. https://doi.org/10.1039/C5RA16328E.